Essays in Biochemistry (2024) **68** 73–82
https://doi.org/10.1042/EBC20230086

Review Article

Catalytic mechanism and kinetics of malate dehydrogenase

Laura de Lorenzo[1], Tyler M.M. Stack[2], Kristin M. Fox[3] and Katherine M. Walstrom[4]

[1]Department of Biochemistry and Molecular Biology, University of New Mexico, School of Medicine, Albuquerque, NM, U.S.A.; [2]Department of Chemistry and Biochemistry, Providence College, Providence, RI, U.S.A.; [3]Department of Chemistry, Union College, Schenectady, NY, U.S.A.; [4]Division of Natural Sciences, New College of Florida, Sarasota, FL, U.S.A.

Correspondence: Katherine M. Walstrom (walstrom@ncf.edu)

Malate dehydrogenase (MDH) is a ubiquitous and central enzyme in cellular metabolism, found in all kingdoms of life, where it plays vital roles in the cytoplasm and various organelles. It catalyzes the reversible NAD^+-dependent reduction of L-malate to oxaloacetate. This review describes the reaction mechanism for MDH and the effects of mutations in and around the active site on catalytic activity and substrate specificity, with a particular focus on the loop that encloses the active site after the substrates have bound. While MDH exhibits selectivity for its preferred substrates, mutations can alter the specificity of MDH for each cosubstrate. The kinetic characteristics and similarities of a variety of MDH isozymes are summarized, and they illustrate that the K_M values are consistent with the relative concentrations of the substrates in cells. As a result of its existence in different cellular environments, MDH properties vary, making it an attractive model enzyme for studying enzyme activity and structure under different conditions.

Introduction

Malate dehydrogenase (MDH, EC 1.1.1.37) catalyzes the reversible conversion of L-malate ((*S*)-malate) to oxaloacetate, accompanied by the conversion of NAD^+ to NADH + H^+, with the addition of the *pro-R* hydrogen to NAD^+ (Figure 1) [1,2]. This enzyme is highly conserved across all kingdoms of life. Eukaryotes contain cytosolic MDH as well as isozymes that are specifically transported to organelles, including mitochondria, chloroplasts, peroxisomes, and glyoxysomes. Although the size of MDH varies among organisms and organelles, MDH is approximately 36 kDa and most commonly functions as a dimer. For NADH produced by cytosolic MDH, reducing equivalents in the form of L-malate allows for the net import of NADH into the mitochondria via the L-malate-aspartate shuttle to drive the production of ATP.

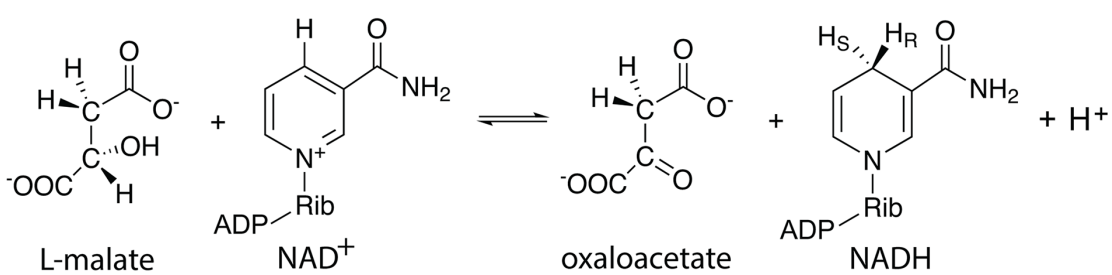

Figure 1. Overall reaction catalyzed by malate dehydrogenase

The illustrated reaction involves the conversion of L-malate to oxaloacetate, accompanied by the reduction of NAD^+ to NADH + H^+. Rib: Ribose, H_S: *pro-S* hydrogen, H_R: *pro-R* hydrogen.

Received: 04 March 2024
Revised: 20 April 2024
Accepted: 23 April 2024

Version of Record published: 03 October 2024

Essays in Biochemistry (2024) **68** 73–82
https://doi.org/10.1042/EBC20230086

Mitochondrial MDH catalyzes an essential step in producing oxaloacetate in the citric acid cycle, in addition to NADH for making ATP.

The active site of MDH features a crucial His 177-Asp 150 pair [3] (this review uses the amino acid numbering for *Escherichia coli* MDH, Uniprot P61889). His 177 forms a hydrogen bond to the hydroxyl group of L-malate, facilitating its conversion to oxaloacetate by removing the hydroxyl proton (Figure 2). L-Malate is oriented in the active site by forming salt bridges between its C1 and C4 carboxylate and Arg 153 and Arg 81, respectively. As described below in more detail, the two substrates bind, and then a flexible loop bearing Arg 81 and a third essential Arg residue, Arg 87, encloses the active site before the reaction proceeds.

Reaction thermodynamics

The equation below represents the reaction catalyzed by MDH, along with the corresponding definition for $K_{eq}^{'}$:

$$\text{L-Malate} + \text{NAD}^+ \rightleftharpoons \text{Oxaloacetate} + \text{NADH} + \text{H}^+ \qquad K_{eq}^{'} = \frac{[Oxaloacetate]\,[NADH]}{[L-Malate]\,[NAD^+]}$$

The observed equilibrium constant for MDH greatly favors the formation of L-malate and NAD^+. Under near-physiological conditions (38°C, pH 7.0, ionic strength $I = 0.25$, 1 mM Mg^{2+}), $K_{eq}^{'} = 2.9 \times 10^{-5}$, corresponding to a $\Delta G = +27$ kJ/mol [4]. The endergonic reaction catalyzed by MDH is facilitated within the mitochondrial cellular environment by coupling with downstream metabolic pathways. NADH is utilized in the electron transport chain to produce ATP, and oxaloacetate is a critical intermediate in the citric acid cycle. The enzyme citrate synthase is energetically favored and consumes the produced oxaloacetate, driving the MDH-catalyzed reaction forward. In laboratory settings, the exergonic reverse reaction (conversion of oxaloacetate to L-malate) is often studied.

As described below, the L-malate oxidation reaction is more favorable at high pH than the oxaloacetate reduction reaction. K_{eq} increases with rising pH levels, reaching $K_{eq}^{'} = 9.1 \times 10^{-4}$ at pH 9 [5]. Despite this increase, the equilibrium still greatly favors oxaloacetate reduction, with the equilibrium percentage of oxaloacetate decreasing slightly from 99.8% at pH 7 to 97.1% at pH 9. Computational modeling of the MDH-catalyzed oxidation of L-malate suggests two distinct steps, each characterized by its own transition states. Initially, His 177 of the *E. coli* MDH deprotonates the hydroxyl group of L-malate with a calculated activation energy $\Delta G^{\ddagger}$ of +29 kJ/mol (Figure 3). Subsequently, the hydride anion from the C2 of L-malate can transfer to NAD^+, representing the rate-limiting catalytic step with a calculated $\Delta G^{\ddagger}$ of +63 kJ/mol [6].

Exploring the role of the substrate binding loop in enzyme catalysis

The catalytic dyad and one substrate binding residue, Arg 153, provide initial contacts with L-malate/oxaloacetate, followed by further interactions with a mobile loop between β4 and α4 (residues 76-88), located near the L-malate/oxaloacetate binding site. This loop includes Arg 81 and Arg 87, which interact with the C4 carboxylate and stabilize the anionic transition state, respectively [7]. The structure of MDH from the archaeon *Metallosphaera sedula* was determined in the presence and absence of NAD^+/L-malate [8]. The active site loop is disordered with high crystallographic temperature factors when no substrate is present and becomes more ordered when the substrate binds (Figure 4). In the structure of the enzyme from *M. sedula* with and without NAD^+, the loop is most open in the apoenzyme. When NAD^+ binds, the loop partially closes, and then completely closes when L-malate binds. On average, the loop moves 6.8 Å between the most open and most closed forms. Molecular dynamics simulations of *Thermus thermophilus* MDH revealed increased mobility of the active site loop at higher simulated temperatures, while the mobility of other loops in the enzyme did not change with temperature [9].

The loop conformations of the MDH enzymes from *Chlorobium vibrioforme* and *Chloroflexus aurantiacus*, adapted to mesophilic and thermophilic environments, respectively, were studied by molecular dynamics simulations [10]. The MDH from the thermophile exhibited more salt bridges, leading to the stabilization of the active site loop by residues even in the absence of substrate. This suggests that the loop is less mobile in the thermophile.

Effect of loop mutations on MDH activity

MDH displays a high level of substrate discrimination, showing a six order of magnitude difference in the reduction rate of oxaloacetate compared to pyruvate. This specificity arises from charge balancing between substrates and the active site of MDH [11]. The activated complex formed upon oxaloacetate and NADH binding includes a positively charged imidazolium ion acting as a general acid, along with two negative charges contributed by each carboxylate

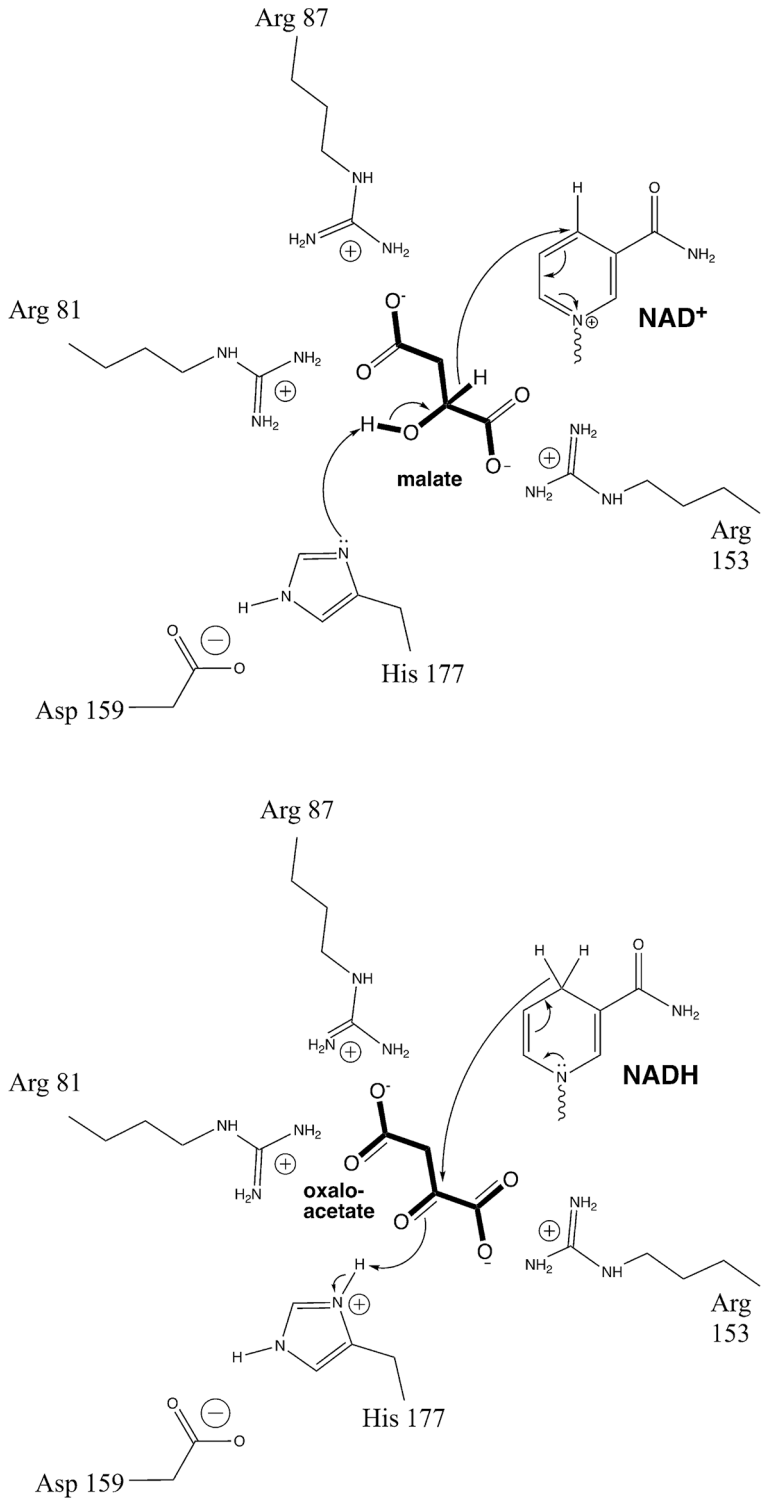

Figure 2. Reaction mechanism for malate dehydrogenase

The diagram on the top illustrates the mechanism of oxidation of L-malate, while the diagram on the bottom is the reverse, the reduction of oxaloacetate.

Essays in Biochemistry (2024) **68** 73–82
https://doi.org/10.1042/EBC20230086

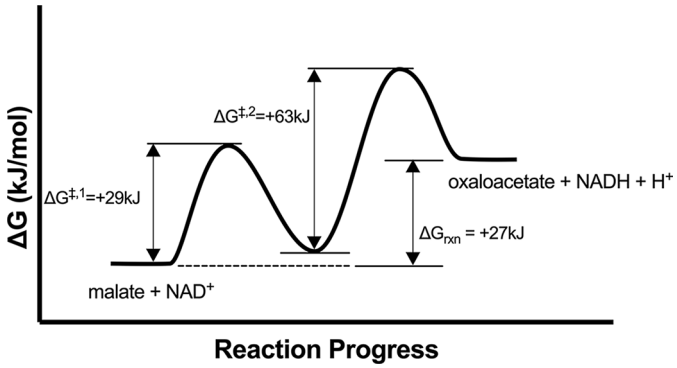

Figure 3. Free energy diagram for MDH

The reaction profile for conversion of malate to oxaloacetate is shown using thermodynamic data from [4,6].

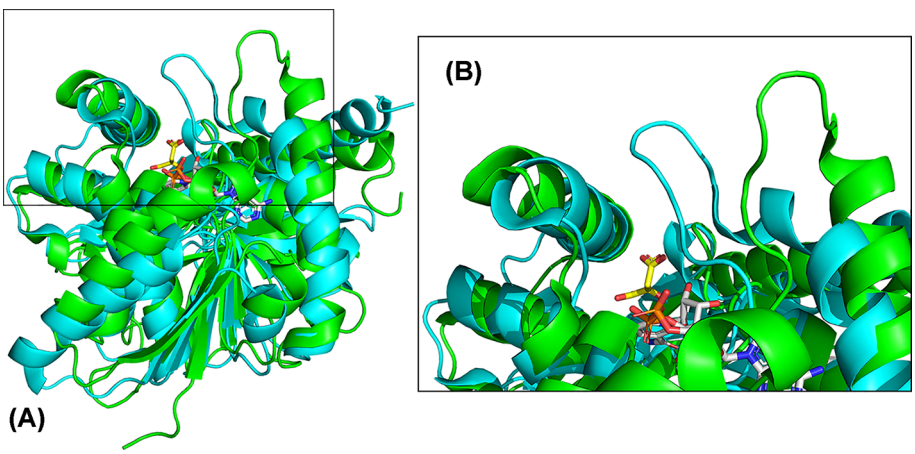

Figure 4. Movement of active site loop upon NAD^+ and L-malate binding to MDH

(**A**) Overall loop movement with open in green (4kde) and closed in cyan (6ihe). (**B**) Close-up of loop movement. L-Malate is shown in sticks with yellow carbons, and NAD^+ is shown in sticks with gray carbons.

of oxaloacetate, resulting in a net negative charge of -1. When oxaloacetate binds, the two loop Arg residues (81 and 87) are driven into close proximity to each other and the C4 carboxylate of oxaloacetate. As pyruvate lacks this complementary negative charge of oxaloacetate, charge repulsion prevents a catalytically productive conformation, leading to the 10^6-fold discrimination [11].

Given the critical role of the active site loop in substrate binding, it is noteworthy that Arg 81 emerges as a key determinant for substrate specificity. In contrast, the related lactate dehydrogenase (LDH) has a Gln residue at the corresponding position. LDH has detectable activity with oxaloacetate, while MDH has comparatively little detectable activity with pyruvate. Mutating the Gln of LDH to an Arg at the corresponding position is critical in creating an LDH that is more specific for oxaloacetate than pyruvate [12]. Conversely, mutating this arginine to glutamine (R81Q) in MDH results in higher specificity for pyruvate, but significantly lower activity than wild-type MDH with oxaloacetate. However, this activity can be improved with other loop mutations; notably, the mutation of the nearby Ala 80 to proline results in a four-fold increase in k_{cat}/K_M [13]. Due to the critical role of loop residues in conferring specificity and the tendency for enzymes with loop mutations to retain some activity, the loop has become a subject of study in Course-based Undergraduate Research Experiences [14].

Furthermore, other mutations in MDH have been found to impact its activity. For instance, the R102Q mutation induces loop closure in *E. coli* MDH, enhancing thermal stability [15]. Mutation of the Arg 153 residue that binds to the C1 carboxylate of the substrate to Cys (R153C) results in a mutant with diminished catalytic activity, although K_M values for L-malate and oxaloacetate remain unaffected [16]. Some mutations, such as Q11G and N119G in *Plasmodium falciparum* MDH, lead to the loss of critical hydrogen bonding interactions with NADH and an increased K_M for oxaloacetate compared with the wild-type [17].

Human MDH2 shows at least three orders of magnitude greater activity with oxaloacetate compared with the longer diacid substrate, α-ketoglutarate. Despite this reduced activity, MDH2 may contribute to the production of 2-hydroxyglutarate in cancer cells. Notably, as the pH is lowered from 7.4 to 6.8, commonly associated with the hypoxic conditions of cells, the generation of 2-hydroxyglutarate by MDH increases while oxaloacetate reduction decreases over the same pH change [18].

Cosubstrate specificity in MDH

MDH generally prefers NAD^+ over $NADP^+$, although $NADP^+$-dependent MDH enzymes do exist in chloroplasts [19]. Cosubstrate specificity is determined by interactions in the β2-loop-α3 region (residues 34-38 in *E. coli* MDH). The cytoplasmic *Thermus thermophilus* (UniProt ID P10584, formerly *Thermus flavus*) MDH efficiently reduces oxaloacetate using both NADH and NADPH, with a 22-fold higher value of k_{cat}/K_M with NADH (8.5×10^7 M^{-1} s^{-1} and 3.9×10^6 M^{-1} s^{-1}, respectively), along with a 14-fold lower K_M value for NADH [20].

Mutation of the β2-loop-α3 region in *T. thermophilus* (amino acids 42-48) to the corresponding residues in chloroplastic *Zea mays* MDH (UniProt ID P15719, amino acids 127-133) leads to a 7-fold increase in efficiency using NADPH as a cosubstrate and a 71-fold decrease when using NADH. Part of the decrease in the K_M for NADPH utilization may be due to the mutation of a Gln to Arg causing ionic attraction with the phosphate of NADPH. However, mutation of other residues in the loop improves the relative efficiency of NADPH-dependent reduction of oxaloacetate [20]. In *Bacillus subtilis*, substituting these same residues converts the wild-type MDH, with a 200-fold preference for NADH, into a mutant enzyme with a 9-fold preference for NADPH. Additionally, this mutant displayed a lower K_M value, higher k_{cat}, and higher k_{cat}/K_M values for NADPH than wild-type NADPH-dependent MDHs from *T. flavus* and *Corynebacterium glutamicum* [21]. The ability to alter the coenzyme specificity of *B. subtilis* MDH from NADH to NADPH opens up new possibilities for utilizing this enzyme in industrial processes that require NADPH-dependent reactions. Understanding the impact of mutations on protein-ligand binding affinity and kinetics is crucial, and computational methods offer valuable insights into MDH mutational dynamics to predict these effects [22].

The Rossman fold found in MDH is common to many nucleotide-binding enzymes, including *S*-adenosyl methionine (SAM)-dependent enzymes. Although *E. coli* MDH has no detectable affinity for SAM, removing three amino acids (ΔAla9, ΔGly10, ΔGln14) from the V/IxGxxGxxG motif found in the β1-loop-α1 region of *E. coli* MDH to create instead a V/IGxGxG motif, typically found in SAM binding Rossman folds, leads to an MDH that binds SAM ($K_d = 13$ μM) and has no observable binding to NAD^+ [23]. These deletions shorten the α1 helix and flatten the loop, expanding the active site to bind SAM.

MDH kinetic parameters

Steady-state enzyme kinetics data are available for both the forward and reverse reactions of many MDH isozymes from various organisms (Table 1). Older experiments often used racemic mixtures of L- and D-malate, and the table indicates when the L enantiomer was utilized. The typical reaction conditions for assays with oxaloacetate included 30–100 mM Tris or phosphate buffer, pH 7–8, with 0–100 mM KCl or NaCl at 30–37°C. As described in this review, enzyme assays using L-malate as a substrate were frequently conducted at a higher pH. For most enzymes, the K_M for oxaloacetate is lower than for L-malate, and the K_M for NADH is lower than for NAD^+, which is reasonable given the lower cellular concentrations of oxaloacetate and NADH compared to L-malate and NAD^+, respectively [24]. The k_{cat} values for L-malate oxidation were much smaller than for oxaloacetate reduction, with MDH from *P. falciparum* exhibiting the highest k_{cat} for L-malate oxidation [25].

Kinetic diversity across MDH isoforms in cellular organelles

When kinetic constants were available for both the cytoplasmic and mitochondrial isozymes in the same organism, the K_M values for oxaloacetate were often similar. However, the K_M for NADH varied, with higher values observed for the mitochondrial isozyme in most cases, as seen in *Caenorhabditis elegans* [36]. This observation is consistent with the higher NADH concentration found in the mitochondria (reviewed in [42]). The chloroplastic MDH from *Arabidopsis thaliana* also had a higher $K_M$for NADH compared to the cytosolic enzyme [34,35]. The K_M values for NADH from different steady-state kinetics experiments with *Sus scrofa* isoforms were more varied [30,32]. Detailed time-course measurements and kinetic models for both cytosolic and mitochondrial *S. scrofa* MDH isoforms predicted higher activity for cytosolic MDH at lower NADH concentrations [43], suggesting that the cytosolic MDH also has a lower K_M for NADH. This comprehensive understanding of MDH kinetics across diverse cellular contexts underscores the adaptability and crucial role of MDH in cellular metabolism.

Essays in Biochemistry (2024) **68** 73–82
https://doi.org/10.1042/EBC20230086

Table 1 Kinetic constants for a variety of purified MDH isozymes

Organism	UniProtKB unique entry	Substrate	K_M (μM)	k_{cat} (s^{-1})	k_{cat}/K_M ($M^{-1}s^{-1}$)	Citation
H. sapiens (cyto*)	P40925-1	OAA	33.4 ± 0.2	200 ± 20	6×10^6	[26]
		OAA	58 ± 12			[27]
		NADH	14.3 ± 1.5	N.D.		
		L-Malate	660 ± 230			
		NAD^+	39 ± 14			
S. scrofa (cyto)	P11708	OAA	30	475	1.36×10^7	[28–30]
		OAA	35 ± 2			
		OAA	8.3 ± 0.6			
		NADH	21 ± 1			
S. scrofa (mito)	P00346	OAA	18, 35	N.D.	N.D.	[30–32]
		NADH	38, 15			
		L-Malate	370, 1100			
		NAD^+	230, 480			
C. vulgaris (mito)	P17783	OAA	150	N.D.	N.D.	[33]
		NADH	110			
		L-Malate	3690			
		NAD^+	460			
C. vulgaris (glyox)	P19446	OAA	180	N.D.	N.D.	[33]
		NADH	130			
		L-Malate	7180			
		NAD^+	460			
A. thaliana (cyto)	P93819	OAA	238 ± 21	608 ± 22	2.6×10^6	[34]
		NADH	72 ± 7	677 ± 24	9.0×10^6	
A. thaliana (chloro)	Q9SN86	OAA	324 ± 109	9.9 ± 1.4	3.1×10^4	[35]
		NADH	431 ± 28	13 ± 9	3.2×10^4	
C. elegans (cyto)	Q9UAV5	OAA	54 ± 4			[36]
		NADH	61 ± 6	350 ± 21	5.7×10^6	
C. elegans (mito)	O02640	OAA	52 ± 4			[36]
		NADH	107 ± 5	460 ± 23	4.3×10^6	
P. falciparum	Q6VVP7	OAA	30 ± 1	960 ± 70	3.2×10^7	[25]
		NADH	36 ± 2	950 ± 80	2.6×10^7	
		L-Malate	1350 ± 24	250 ± 19	1.8×10^5	
		NAD^+	152 ± 13	150 ± 20	9.8×10^5	
E. coli	P61889	OAA	40-50	900-930	2.3×10^7	[37,38]
		NADH	61 ± 2			
		L-Malate	2600 ± 200	21	8.1×10^3	
		NAD^+	260 ± 30			
T. thermophilus	P10584	OAA	9.8	N.D.	N.D.	[39]
		NADH	6			
		L-Malate	26			
		NAD^+	19			
S. coelicolor	Q9K3J3	OAA	189	1870	1×10^4	[40]
		NADH	83	542	6.56×10^3	
		L-Malate	494	4.71	9.53	
		NAD^+	150	3.66	24.4	
H. marismortui	Q07841	OAA	130	N.D.	N.D.	[41]
		NADH	12			

*chloro, chloroplastic; cyto, cytosolic; glyox, glyoxysomal; mito, mitochondrial; N.D., not done in the published article; OAA, oxaloacetate.

MDH kinetics and environmental factors

MDH follows an ordered Bi-Bi kinetic mechanism characterized by the sequential binding of NAD^+ and then L-malate, followed by the release of oxaloacetate and then NADH [5,43–46]. The kinetic evidence supports a compulsory order reaction mechanism, and some studies suggest that an enzyme isomerization is involved [47–49]. Lodola et al. found that dimeric MDH has two independent active sites that can function simultaneously [50].

Generally, MDH activity has an optimal temperature range between 30 and 40°C. Deviations from this range are somewhat related to the organism's physiological temperature range. Thermostability also varies among MDH isoforms, with cytosolic isoforms being more stable than mitochondrial isoforms, such as in *C. elegans* [36], *S. scrofa* [28,51,52], and *Sphyraena idiastes* [30]. However, these enzymes from eukaryotic species are notably less stable than MDH from the mesophile *Streptomyces coelicolor* and the thermophilic bacterium *T. thermophilus*. *S. coelicolor* MDH remains active at 50°C but rapidly inactivates above this temperature, while *T. thermophilus* MDH retains activity at 90°C for 60 min [20,39,40,51]. A larger number of salt bridges between subunits contributes to thermal stability [28,53]. However, thermal stability is a complex trait influenced by multiple factors, including electrostatic interactions, hydrophobic interactions, hydrogen bonding, and overall protein folding [28,53–55].

Optimal enzyme activity is achieved when MDH reduces oxaloacetate near pH 8, and activity is generally high from pH ∼7–8.5 [5,21,36,56]. Interestingly, the optimal pH for some thermostable MDHs varies with temperature [39,40]. The L-malate oxidation rate is higher at pH > 8 [25,39,43,56]. The pH-dependency of MDH kinetic behavior involves additional ionic states and still follows the ordered Bi-Bi mechanism but is modified to account for enzyme protonation states [5,43,57]. The mitochondrial porcine MDH binds a proton on a His residue upon binding to NADH [58], and a His is deprotonated before L-malate binds [1]. This is consistent with the active site base, His 177, having the appropriate protonation state in each catalytic direction. Also, the interaction of NAD^+ with MDH was dependent on the protonation of two unidentified residues, with pK_a values of ∼6 and 7–8 [5,43].

MDH regulation

Excessive oxaloacetate inhibits cytoplasmic and mitochondrial MDH, but at concentrations too high to influence enzyme activity in the cell [29,59]. Interestingly, oxaloacetate may also inhibit NAD^+ binding, potentially with greater potency than its impact on NADH [47]. L-malate activates MDH at a site that is different from the active site [31,46]. Additionally, citrate is an allosteric regulator of MDH, and the influence of citrate on MDH activity is intricate and multifaceted. Citrate-activated mitochondrial MDH (mMDH) promotes the oxidation of L-malate [48], and this may be another mechanism to promote this energetically unfavorable reaction. However, citrate inhibited oxaloacetate reduction by mMDH and in both directions of the reaction by cytoplasmic MDH (cMDH) [48]. Interestingly, it was later found that citrate only activated mMDH when L-malate and NAD^+ concentrations were elevated (2.5–10 mM and 1–5 mM, respectively), while citrate inhibited L-malate oxidation at low concentrations of L-malate or NAD^+ [49]. All three effectors (oxaloacetate, L-malate, and citrate) bind to the same putative allosteric site [48].

Human mMDH is an allosteric enzyme that interacts cooperatively with L-malate, with tetramers showing higher activity than dimers [60]. When using NADH as a cofactor, human mMDH is activated by fumarate that binds at the dimer interface at a site ∼30 Å from the active site [60]. The enzyme is also inhibited by ATP, which binds to a site at the tetramer interface (also called the exosite) where ATP/ADP and NAD^+/NADH can bind. The binding of ATP leads to the dimer being more stable than the tetramer, causing inhibition [61]. ADP has a similar but much weaker effect. The binding of NAD^+ to the tetramer interface leads to the tetramer being more stable and increased activity. Other mammalian MDH enzymes (cMDH and mMDH-$NADP^+$) have not been shown to be similarly regulated.

Summary

- *In vivo*, the reaction catalyzed by malate dehydrogenase mainly proceeds in the direction of L-malate oxidation, but in the lab, it is easier to study the reaction in the spontaneous reverse direction.
- MDH is present in all known organisms, and there are different isozymes in organelles.
- Multiple investigations of the flexible active site loop and other residues have shown that MDH is a good model system for investigating the basis of substrate specificity.
- Regulation of MDH is complex, and the enzyme is affected allosterically by several molecules.

Essays in Biochemistry (2024) **68** 73–82
https://doi.org/10.1042/EBC20230086

- There is little published work on human MDH, which may be a fruitful area of future study.

Competing Interests

The authors declare that there are no competing interests associated with the manuscript.

Abbreviations

$\Delta G^{\ddagger}$, activation energy; *A. thaliana*, *Arabidopsis thaliana*; ATP, adenosine triphosphate; *C. elegans*, *Caenorhabditis elegans*; *C. vulgaris*, *Citrullus vulgaris*; chloro, chloroplastic; cMDH, cytoplasmic malate dehydrogenase; cyto, cytoplasmic; *E. coli*, *Escherichia coli*; glyox, glyoxosomal; *H. marismortui*, *Haloarcula marismortui*; *H. sapiens*, *Homo sapiens*; kDa, kilodalton; *M. sedula*, *Metallosphaera sedula*; MDH, malate dehydrogenase; mito, mitochondrial; mMDH, mitochondrial malate dehydrogenase; NAD^+, nicotinamide adenine dinucleotide; NADH, dihydronicotinamide adenine dinucleotide; $NADP^+$, nicotinamide adenine dinucleotide phosphate; NADPH, dihydronicotinamide adenine dinucleotide phosphate; OAA, oxaloacetate; *P. falciparum*, *Plasmodium falciparum*; *S. coelicolor*, *Streptomyces coelicolor*; *S. scrofa*, *Sus scrofa*; SAM, *S*-adenosyl methionine; *T. thermophilus*, *Thermus thermophilus* (formerly *Thermus flavus*).

References

1 Bernstein, L.H. and Everse, J. (1978) Studies on the mechanism of the malate dehydrogenase reaction. *J. Biol. Chem.* **253**, 8702–8707, https://doi.org/10.1016/S0021-9258(17)34234-5
2 Oppenheimer, N.J. (1986) The stereospecificity of oxidation of alpha-[4R-2H]NADH by dehydrogenases. *J. Biol. Chem.* **261**, 12209–12212, https://doi.org/10.1016/S0021-9258(18)67225-4
3 Birktoft, J.J. and Banaszak, L.J. (1983) The presence of a histidine-aspartic acid pair in the active site of 2-hydroxyacid dehydrogenases. X-ray refinement of cytoplasmic malate dehydrogenase. *J. Biol. Chem.* **258**, 472–482, https://doi.org/10.1016/S0021-9258(18)33280-0
4 Guynn, R.W., Gelberg, H.J. and Veech, R.L. (1973) Equilibrium constants of the malate dehydrogenase, citrate synthase, citrate lyase, and acetyl coenzyme A hydrolysis reactions under physiological conditions. *J. Biol. Chem., Elsevier* **248**, 6957–6965, https://doi.org/10.1016/S0021-9258(19)43346-2
5 Dasika, S.K., Vinnakota, K.C. and Beard, D.A. (2015) Determination of the catalytic mechanism for mitochondrial malate dehydrogenase. *Biophys. J., Elsevier* **108**, 408–419, https://doi.org/10.1016/j.bpj.2014.11.3467
6 Cunningham, M.A., Ho, L.L., Nguyen, D.T., Gillilan, R.E. and Bash, P.A. (1997) Simulation of the enzyme reaction mechanism of malate dehydrogenase. *Biochemistry* **36**, 4800–4816, https://doi.org/10.1021/bi962734n
7 Hall, M.D. and Banaszak, L.J. (1993) Crystal structure of a ternary complex of *Escherichia coli* malate dehydrogenase citrate and NAD at 1.9 Å resolution. *J. Mol. Biol.* **232**, 213–222, https://doi.org/10.1006/jmbi.1993.1377
8 Lee, D., Hong, J. and Kim, K.-J. (2019) Crystal structure and biochemical characterization of malate dehydrogenase from *Metallosphaera sedula*. *Biochem. Biophys. Res. Commun.* **509**, 833–838, https://doi.org/10.1016/j.bbrc.2019.01.018
9 Hung, C.-H., Hwang, T.-S., Chang, Y.-Y., Luo, H.-R., Wu, S.-P. and Hsu, C.-H. (2013) Crystal structures and molecular dynamics simulations of thermophilic malate dehydrogenase reveal critical loop motion for co-substrate binding. *PLoS ONE* **8**, e83091, https://doi.org/10.1371/journal.pone.0083091
10 Kalimeri, M., Girard, E., Madern, D. and Sterpone, F. (2014) Interface matters: the stiffness route to stability of a thermophilic tetrameric malate dehydrogenase. *PLoS ONE* **9**, e113895, Public Library of Science, https://doi.org/10.1371/journal.pone.0113895
11 Chapman, A.D., Cortés, A., Dafforn, T.R., Clarke, A.R. and Brady, R.L. (1999) Structural basis of substrate specificity in malate dehydrogenases: crystal structure of a ternary complex of porcine cytoplasmic malate dehydrogenase, alpha-ketomalonate and tetrahydoNAD. *J. Mol. Biol.* **285**, 703–712, https://doi.org/10.1006/jmbi.1998.2357
12 Wilks, H.M., Hart, K.W., Feeney, R., Dunn, C.R., Muirhead, H., Chia, W.N. et al. (1988) A specific, highly active malate dehydrogenase by redesign of a lactate dehydrogenase framework. *Science* **242**, 1541–1544, https://doi.org/10.1126/science.3201242
13 Boernke, W.E., Millard, C.S., Stevens, P.W., Kakar, S.N., Stevens, F.J. and Donnelly, M.I. (1995) Stringency of substrate-specificity of *Escherichia coli* malate-dehydrogenase. *Arch. Bioch. Biophys.* **322**, 43–52, https://doi.org/10.1006/abbi.1995.1434
14 Provost, J.J. (2022) Increasing access for biochemistry research in undergraduate education: The malate dehydrogenase CURE community. *J. Biol. Chem.* **298**, 102298, https://doi.org/10.1016/j.jbc.2022.102298
15 Goward, C.R., Miller, J., Nicholls, D.J., Irons, L.I., Scawen, M.D., O'brien, R. et al. (1994) A single amino acid mutation enhances the thermal stability of *Escherichia coli* malate dehydrogenase. *Eur. J. Biochem.* **224**, 249–255, https://doi.org/10.1111/j.1432-1033.1994.tb20018.x
16 Wright, S.K. and Viola, R.E. (2001) Alteration of the specificity of malate dehydrogenase by chemical modulation of an active site arginine. *J. Biol. Chem.* **276**, 31151–31155, https://doi.org/10.1074/jbc.M100892200
17 Pradhan, A., Tripathi, A.K., Desai, P.V., Mukherjee, P.K., Avery, M.A., Walker, L.A. et al. (2009) Structure and function of *Plasmodium falciparum* malate dehydrogenase: Role of critical amino acids in co-substrate binding pocket. *Biochimie* **91**, 1509–1517, https://doi.org/10.1016/j.biochi.2009.09.005
18 Nadtochiy, S.M., Schafer, X., Fu, D., Nehrke, K., Munger, J. and Brookes, P.S. (2016) Acidic pH is a metabolic switch for 2-hydroxyglutarate generation and signaling. *J. Biol. Chem.* **291**, 20188–20197, https://doi.org/10.1074/jbc.M116.738799

19 Ferte, N., Jacquot, J.-P. and Meunier, J.-C. (1986) Structural, immunological and kinetic comparisons of NADP-dependent malate dehydrogenases from spinach (C3) and corn (C4) chloroplasts. *Eur. J. Biochem.* **154**, 587–595, https://doi.org/10.1111/j.1432-1033.1986.tb09439.x
20 Nishiyama, M., Birktoft, J.J. and Beppu, T. (1993) Alteration of coenzyme specificity of malate dehydrogenase from *Thermus flavus* by site-directed mutagenesis. *J. Biol. Chem.* **268**, 4656–4660, https://doi.org/10.1016/S0021-9258(18)53446-3
21 Ge, Y.-D., Guo, Y.-T., Jiang, L.-L., Wang, H.-H., Hou, S.-L. and Su, F.-Z. (2023) Enzymatic characterization and coenzyme specificity conversion of a novel dimeric malate dehydrogenase from *Bacillus subtilis*. *Protein J.* **42**, 14–23, https://doi.org/10.1007/s10930-022-10087-0
22 Wang, D.D., Ou-Yang, L., Xie, H., Zhu, M. and Yan, H. (2020) Predicting the impacts of mutations on protein-ligand binding affinity based on molecular dynamics simulations and machine learning methods. *Comput. Struct. Biotech. J.* **18**, 439–454, https://doi.org/10.1016/j.csbj.2020.02.007
23 Toledo-Patiño, S., Pascarelli, S., Uechi, G. and Laurino, P. (2022) Insertions and deletions mediated functional divergence of Rossmann fold enzymes. *Proc. Natl. Acad. Sci. U.S.A.* **119**, e2207965119, https://doi.org/10.1073/pnas.2207965119
24 Opie, L.H. and Owen, P. (1975) Effects of increased mechanical work by isolated perfused rat heart during production or uptake of ketone bodies. Assessment of mitochondrial oxidized to reduced free nicotinamide-adenine dinucleotide ratios and oxaloacetate concentrations. *Biochem. J.* **148**, 403–415, https://doi.org/10.1042/bj1480403
25 Tripathi, A.K., Desai, P.V., Pradhan, A., Khan, S.I., Avery, M.A., Walker, L.A. et al. (2004) An alpha-proteobacterial type malate dehydrogenase may complement LDH function in *Plasmodium falciparum*. Cloning and biochemical characterization of the enzyme. *Eur. J. Biochem.* **271**, 3488–3502, https://doi.org/10.1111/j.1432-1033.2004.04281.x
26 Cornely, K. and Stack, T. (2024) hMDH1 oxaloacetate kinetic data. *Mendeley Data* **V1**, https://doi.org/10.17632/63myn5n4c8.1
27 Crow, K.E., Braggins, T.J. and Hardman, M.J. (1983) Human liver cytosolic malate dehydrogenase: purification, kinetic properties, and role in ethanol metabolism. *Arch. Biochem. Biophys.* **225**, 621–629, https://doi.org/10.1016/0003-9861(83)90073-5
28 Trejo, F., Gelpí, J.Ll., Ferrer, A., Boronat, A., Busquets, M. and Cortés, A. (2001) Contribution of engineered electrostatic interactions to the stability of cytosolic malate dehydrogenase. *Protein Eng. Des. Sel.* **14**, 911–917, https://doi.org/10.1093/protein/14.11.911
29 Bernstein, L.H., Grisham, M.B., Cole, K.D. and Everse, J. (1978) Substrate inhibition of the mitochondrial and cytoplasmic malate dehydrogenases. *J. Biol. Chem.* **253**, 8697–8701, https://doi.org/10.1016/S0021-9258(17)34233-3
30 Lin, J.-J., Yang, T.-H., Wahlstrand, B.D., Fields, P.A. and Somero, G.N. (2002) Phylogenetic relationships and biochemical properties of the duplicated cytosolic and mitochondrial isoforms of malate dehydrogenase from a teleost fish, *Sphyraena idiastes*. *J. Mol. Evol.* **54**, 107–117, https://doi.org/10.1007/s00239-001-0023-z
31 Telegdi, M., Wolfe, D.V. and Wolfe, R.G. (1973) Malate Dehydrogenase. XII. Initial rate kinetic studies of substrate activation of porcine mitochondrial enzyme by malate. *J. Biol. Chem.* **248**, 6484–6489, https://doi.org/10.1016/S0021-9258(19)43471-6
32 DuVal, G., Swaisgood, H.E. and Horton, H.R. (1985) Some kinetic characteristics of immobilized protomers and native dimers of mitochondrial malate dehydrogenase: an examination of the enzyme mechanism. *Biochemistry* **24**, 2067–2072, https://doi.org/10.1021/bi00329a039
33 Walk, R.-A. and Hock, B. (1977) Glyoxysomal and mitochondrial malate dehydrogenase of watermelon (*Citrullus vulgaris*) cotyledons: II. Kinetic properties of the purified isoenzymes. *Planta* **136**, 221–228, https://doi.org/10.1007/BF00385988
34 Huang, J., Niazi, A.K., Young, D., Rosado, L.A., Vertommen, D., Bodra, N. et al. (2018) Self-protection of cytosolic malate dehydrogenase against oxidative stress in *Arabidopsis*. *J. Exp. Bot.* **69**, 3491–3505, https://doi.org/10.1093/jxb/erx396
35 An, Y., Cao, Y. and Xu, Y. (2016) Purification and characterization of the plastid-localized NAD-dependent malate dehydrogenase from *Arabidopsis thaliana*. *Biotechnol. Appl. Biochem.* **63**, 490–496, https://doi.org/10.1002/bab.1406
36 Thomas, M.J., Cassidy, E.R., Robinson, D.S. and Walstrom, K.M. (2022) Kinetic characterization and thermostability of *C. elegans* cytoplasmic and mitochondrial malate dehydrogenases. *BBA-Proteins Proteom* **1870**, 140722, https://doi.org/10.1016/j.bbapap.2021.140722
37 Yin, Y. and Kirsch, J.F. (2007) Identification of functional paralog shift mutations: conversion of *Escherichia coli* malate dehydrogenase to a lactate dehydrogenase. *Proc. Natl. Acad. Sci. U.S.A.* **104**, 17353–17357, https://doi.org/10.1073/pnas.0708265104
38 Muslin, E.H., Li, D., Stevens, F.J., Donnelly, M., Schiffer, M. and Anderson, L.E. (1995) Engineering a domain-locking disulfide into a bacterial malate dehydrogenase produces a redox-sensitive enzyme. *Biophys. J.* **68**, 2218–2223, https://doi.org/10.1016/S0006-3495(95)80430-3
39 Iijima, S., Saiki, T. and Beppu, T. (1980) Physicochemical and catalytic properties of thermostable malate dehydrogenase from an extreme thermophile *Thermus Flavus AT-62*. *Biochim. Biophys. Acta* **613**, 1–9, https://doi.org/10.1016/0005-2744(80)90185-0
40 Ge, Y.-D., Cao, Z.-Y., Wang, Z.-D., Chen, L.-L., Zhu, Y.-M. and Zhu, G.-P. (2010) Identification and Biochemical Characterization of a Thermostable Malate Dehydrogenase from the Mesophile *Streptomyces coelicolor* A3(2). *Biosci. Biotech. Bioch.* **74**, 2194–2201, https://doi.org/10.1271/bbb.100357
41 Madern, D. and Ebel, C. (2007) Influence of an anion-binding site in the stabilization of halophilic malate dehydrogenase from *Haloarcula marismortui*. *Biochimie* **89**, 981–987, https://doi.org/10.1016/j.biochi.2007.03.008
42 Stein, L.R. and Imai, S. (2012) The dynamic regulation of NAD metabolism in mitochondria. *Trends Endocrinol. Metab.* **23**, 420–428, https://doi.org/10.1016/j.tem.2012.06.005
43 Dasika, S.K., Vinnakota, K.C. and Beard, D.A. (2015) Characterization of the kinetics of cardiac cytosolic malate dehydrogenase and comparative analysis of cytosolic and mitochondrial isoforms. *Biophys. J.* **108**, 420–430, https://doi.org/10.1016/j.bpj.2014.11.3466
44 Silverstein, E. and Sulebele, G. (1969) Catalytic mechanism of pig heart mitochondrial malate dehydrogenase studied by kinetics at equilibrium. *Biochemistry* **8**, 2543–2550, https://doi.org/10.1021/bi00834a042
45 Harada, K. and Wolfe, R.G. (1968) Malic dehydrogenase. VII. The catalytic mechanism and possible role of identical protein subunits. *J. Biol. Chem.* **243**, 4131–4137, https://doi.org/10.1016/S0021-9258(18)93289-8
46 Mueggler, P.A. and Wolfe, R.G. (1978) Malate dehydrogenase. Kinetic studies of substrate activation of supernatant enzyme by L-malate. *Biochemistry* **17**, 4615–4620, https://doi.org/10.1021/bi00615a006

Essays in Biochemistry (2024) **68** 73–82
https://doi.org/10.1042/EBC20230086

47 Heyde, E. and Ainsworth, S. (1968) Kinetic studies on the mechanism of the malate dehydrogenase reaction. *J. Biol. Chem.* **243**, 2413–2423, https://doi.org/10.1016/S0021-9258(18)93490-3
48 Mullinax, T.R., Mock, J.N., McEvily, A.J. and Harrison, J.H. (1982) Regulation of mitochondrial malate dehydrogenase. Evidence for an allosteric citrate-binding site. *J. Biol. Chem.* **257**, 13233–13239, https://doi.org/10.1016/S0021-9258(18)33435-5
49 Gelpí, J.L., Dordal, A., Montserrat, J., Mazo, A. and Cortés, A. (1992) Kinetic studies of the regulation of mitochondrial malate dehydrogenase by citrate. *Biochem. J.* **283**, 289–297, https://doi.org/10.1042/bj2830289
50 Lodola, A., Shore, J.D., Parker, D.M. and Holbrook, J. (1978) Malate dehydrogenase of the cytosol. A kinetic investigation of the reaction mechanism and a comparison with lactate dehydrogenase. *Biochem. J.* **175**, 987–998, https://doi.org/10.1042/bj1750987
51 Duffield, M.L., Nicholls, D.J., Atkinson, T. and Scawen, M.D. (1994) An investigation of the thermal stabilities of two malate dehydrogenases by comparison of their three-dimensional structures. *J. Mol. Graphics* **12**, 14–21, https://doi.org/10.1016/0263-7855(94)80003-0
52 Müller, J. and Klein, C. (1982) Stability of dehydrogenases. III. Malate dehydrogenases. *Biochim. Biophys. Acta* **707**, 133–141, https://doi.org/10.1016/0167-4838(82)90406-X
53 Dalhus, B., Saarinen, M., Sauer, U.H., Eklund, P., Johansson, K., Karlsson, A. et al. (2002) Structural basis for thermophilic protein stability: structures of thermophilic and mesophilic malate dehydrogenases. *J. Mol. Biol.* **318**, 707–721, https://doi.org/10.1016/S0022-2836(02)00050-5
54 Brininger, C., Spradlin, S., Cobani, L. and Evilia, C. (2018) The more adaptive to change, the more likely you are to survive: Protein adaptation in extremophiles. *Seminars Cell Dev. Biol.* **84**, 158–169, https://doi.org/10.1016/j.semcdb.2017.12.016
55 Goldenzweig, A. and Fleishman, S.J. (2018) Principles of protein stability and their application in computational design. *Ann. Rev. Biochem.* **87**, 105–129, https://doi.org/10.1146/annurev-biochem-062917-012102
56 Walk, R.-A., Michaeli, S. and Hock, B. (1977) Glyoxysomal and Mitochondrial Malate Dehydrogenase of Watermelon (*Citrullus vulgaris*) Cotyledons: I. Molecular Properties of the Purified Isoenzymes. *Planta, Springer* **136**, 211–220, https://doi.org/10.1007/BF00385987
57 Raval, D.N. and Wolfe, R.G. (1962) Malic dehydrogenase. IV. pH Dependence of the kinetic parameters. *Biochemistry* **1**, 1118–1123, https://doi.org/10.1021/bi00912a024
58 Hodges, C.T., Jurgensen, S.R. and Harrison, J.H. (1980) Investigation of the pH dependence of proton uptake by porcine heart mitochondrial malate dehydrogenase upon binding of NADH. *Arch. Biochem. Biophys.* **203**, 580–586, https://doi.org/10.1016/0003-9861(80)90215-5
59 Raval, D.N. and Wolfe, R.G. (1963) Malic dehydrogenase. V. Kinetic studies of substrate inhibition by oxalacetate. *Biochemistry* **2**, 220–224, https://doi.org/10.1021/bi00902a003
60 Hung, H.-C., Kuo, M.-W., Chang, G.-G. and Liu, G.-Y. (2005) Characterization of the functional role of allosteric site residue Asp102 in the regulatory mechanism of human mitochondrial NAD(P)+-dependent malate dehydrogenase (malic enzyme). *Biochem. J.* **392**, 39–45, https://doi.org/10.1042/BJ20050641
61 Hsieh, J.-Y., Shih, W.-T., Kuo, Y.-H., Liu, G.-Y. and Hung, H.-C. (2019) Functional roles of metabolic intermediates in regulating the human mitochondrial NAD(P)+-dependent malic enzyme. *Sci. Rep.* **9**, 9081, https://doi.org/10.1038/s41598-019-45282-0